Journal Pre-proof

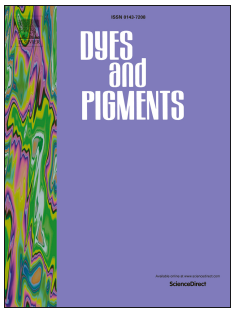

Influence of the *meso*-substituents of zinc porphyrins in dye-sensitized solar cell efficiency with improved performance under short periods of white light illumination

Joana M.D. Calmeiro, Gabriel Gira, Francisco M. Ferraz, Sara R.G. Fernandes, Ana L. Pinto, Leandro M.O. Lourenço, João P.C. Tomé, Cláudia C.L. Pereira

PII: S0143-7208(19)32984-5

DOI: https://doi.org/10.1016/j.dyepig.2020.108280

Reference: DYPI 108280

To appear in: *Dyes and Pigments*

Received Date: 19 December 2019

Revised Date: 11 February 2020

Accepted Date: 11 February 2020

Please cite this article as: Calmeiro JMD, Gira G, Ferraz FM, Fernandes SRG, Pinto AL, Lourenço LMO, Tomé JoãPC, Pereira CláCL, Influence of the *meso*-substituents of zinc porphyrins in dye-sensitized solar cell efficiency with improved performance under short periods of white light illumination, *Dyes and Pigments* (2020), doi: https://doi.org/10.1016/j.dyepig.2020.108280.

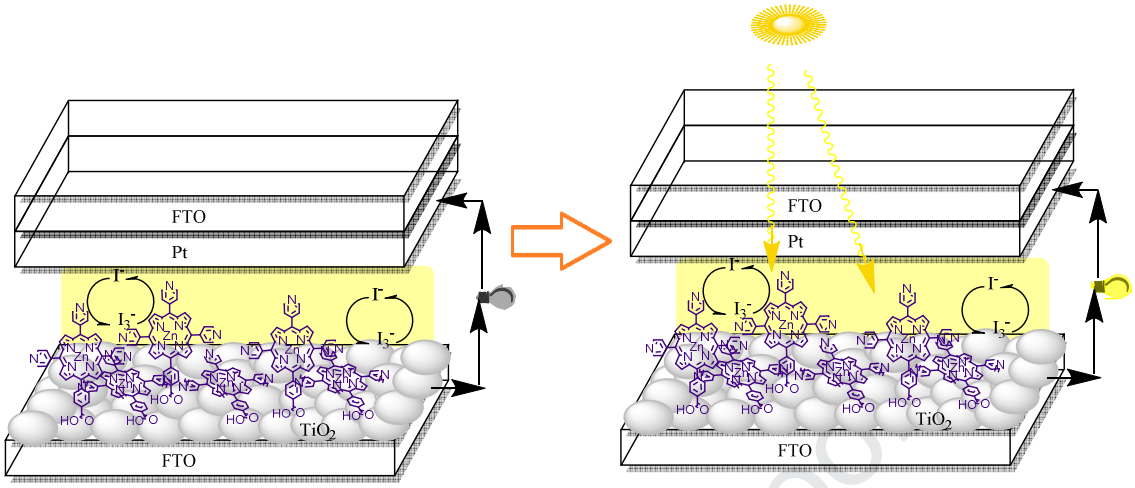

Influence of the *meso*-substituents of Zinc Porphyrins in Dye-Sensitized Solar Cell Efficiency with Improved Performance under Short Periods of White Light Illumination

Authors: Joana M. D. Calmeiro[a,b], Gabriel Gira[b,c], Francisco M. Ferraz[b,c], Sara R. G. Fernandes[b], Ana L. Pinto[c], Leandro M. O. Lourenço[a*], João P. C. Tomé[b*], Cláudia C. L. Pereira[c*]

[a] *LAQV-REQUIMTE, Chemistry Department, University of Aveiro, 3810-193 Aveiro, Portugal.*

[b]*Centro de Química Estrutural, Departamento de Engenharia Química, Instituto Superior Técnico, Universidade de Lisboa, Av Rovisco Pais, 1049-001 Lisboa, Portugal.*

[c]*LAQV-REQUIMTE, Departamento de Química, Faculdade de Ciências e Tecnologia, Universidade NOVA de Lisboa, 2829-516 Caparica, Portugal.*

Abstract:

The sensitization activity of four zinc metalloporphyrin dyes: *meso*-tetrakis(4-pyridyl)porphyrinato Zn(II) (**a**), *meso*-triphenyl-(4-carboxyphenyl)porphyrinato Zn(II) (**b**), *meso*-tetrakis(4-carboxyphenyl)porphyrinato Zn(II) (**c**) and *meso*-tripyridyl(4-carboxyphenyl)porphyrinato Zn(II) (**d**) is reported here, in terms of current-potential curve, open-circuit potential, fill factor, and overall solar energy conversion efficiency which have been evaluated under 100 mW/cm^2 light intensity and their performances compared to the benchmark

N719 (di-tetrabutylammonium *cis*-bis(isothiocyanato)bis(2,2′-bipyridyl-4,4′-dicarboxylato) ruthenium(II). This work focus the structural aspects of dyes with anchoring groups using TiO_2-based Dye Sensitized Solar Cells (DSSCs), which includes pyridyl and carboxyphenyl acid groups and argue how the combination of both anchoring groups, in the same structure, may allow relevant optimization of DSSCs performance in the near future.

Also, a noticeable improvement in the photovoltaic performance of all dyes, reaching a maximum increase from 25% to 69% in the overall DSSC efficiency under short periods of white light illumination is discussed.

Keywords:

Dye sensitized solar cells (DSSCs); Metalloporphyrin; Dyes; Macrocycles; Carboxylic acid anchoring group; TiO_2; Photoconversion efficiency.

Introduction:

In 2005, the worldwide electricity generation was of 17 450 TWh, out of which 40% came from coal, 20% from gas, 16% from nuclear, 16% from hydro source, 7% from oil and only ~2% was originated from renewable resources such as solar, wind, geothermal, waste and renewable combustible.[1] In 2017, the energy generation from combustible fuels (coal, oil, natural gas, biofuel, biomass, industrial waste and municipal waste) accounted for 66.8% of total world gross electricity production, and the solar energy alone, in the same year produced about 1.8% of total solar energy, wind energy produced 4.4% and relatively to geothermal energy 0.5%. In 2018, according to global energy statistical year board, the electricity production was of 74% of non-renewable energy and 26% from renewable energy.[2]

Solar energy seems to be the best renewable technology to be adopted for electricity generation; it has a lesser impact on environment, less land requirement and higher public acceptance.

In this way, dye-sensitized solar cells (DSSCs) is presented as a technically and economically credible alternative concept for light harvesting. Dye sensitized solar cells are generally comprised of a photoanode which is made of a semiconductor (e.g. TiO_2), photo-sensitizer (dye molecules[3]) deposited on transparent semi-conducting oxide substrate and hole conducting material as electrolyte.[4] Therefore, donor–acceptor assemblies also play key roles in molecular photovoltaic devices[5], where energy is stored in the photogenerated radical ion pair states and then converted into electrical power.

The solar-light-converting systems methodology for photo-electrical conversion DSSCs is bio-inspired in structures that exist in Nature, where organisms developed an efficient strategy to improve light capture by using special molecular units called light harvesting antennas.[6] One example of bio-inspired photosensitizers are anthocyanins with great potential to be used in DSSCs.[7-9] An overall efficiency of 1.15% was obtained for the compound, 10-catecholpyrano-5,7,3′,4′-tetrahydroxyflavylium, clearly showing that the presence of catechol unit increases electron injection to the TiO_2 semiconductor.[8] Pyranoanthocyanins, present in red wine, display also great potential as photosensitizers in bio-inspired DSSCs. An overall efficiency of 1.57% was obtained for the best performing compound, methylpyranocyanidin-3-*O*-glucoside, results that are comparable to what is found in the literature for naturally occurring compounds, such has anthocyanins extracted from eggplants.[10]

Metalloporphyrins are present in nature as a *heme* cofactor of haemoglobins, cytochromes and other active redox enzymes, and metallochlorins, more saturated analogues, are present in the photosynthetic apparatus of plants and bacteria. ZnPor derivatives have been studied and

considered a challenge for the scientific community as promising electron donors, which promoted the grown interest on them as attractive and alternative dyes for DSSCs. Their properties like high stabilities, great absorption coefficients in the ultraviolet-visible (UV-Vis) and near infrared (IR) regions, tunable redox and photophysical features, moderated cost and environmentally friendly make them unique for DSSC preparation.[11] Indeed, a common DSSC comprises a sensitizing dye chemically linked, for example, by a carboxylic acid anchoring group[12] to a nanocrystalline wide band gap semiconductor, such as thin films of TiO_2, ZnO or SnO_2.[13] Their electronic properties are centered toward light induced charge transfer at a nanoparticle metal oxide/dye/electrolyte interface,[14] where the conversion process depends on the efficiency of electrons injection from the excited state of the dye to the acceptor states of the metal oxide conduction band, the dye regeneration and the recombination reactions.[15] Therefore, strong effort has been made to the progressive development of metalloporphyrin sensitizers with well-defined design and representative electron conductors as donor-acceptor frameworks.[16]

As already stated, porphyrins, as sensitizers, have favorable spectral characteristics like strong absorption in the visible region, but also several reaction sites available for structural modification. They are one of the most widely studied organic-based dyes for DSSCs owing to their extremely intense Soret band at 400−450 nm and intense Q bands at 550−600 nm;[17] although their relatively small bandwidth and lack of absorption in the 450−550 nm and 650−900 nm visible ranges, represent one of the limiting factors of these dyes in DSSCs.

As refereed above, intrinsic photon capturing and associated photo-induced electron transfer properties, typical of porphyrin macrocycle, extimulated the idea of using these compounds as antennae in ‘artificial photosynthesis’.[18] The porphyrins core metallization greatly alters some of their physicochemical properties, such as: absorption, fluorescence and solubility. Several

efficient porphyrin sensitizers have been reported by Grätzel, Diau, Yeh, Lin, Wang, Imahori, and many other groups.[19]

So far, the best conventional efficiencies have been obtained with ruthenium-based porphyrins using an electrolyte based on iodide/triiodide redox couple. Zn(II) metalloporphyrin have shown to be the most efficient porphyrin photosensitizer tested to date, and it offers potential alternative to Ru-based dyes in the DSSCs.[20]

Grätzel and coworkers developed 2,1,3-benzothiadiazole (BTD) as a π-conjugated linker between the anchoring group and porphyrin system to fill the void between the Soret and Q bands in the absorption spectrum allowing a photoconversion efficiency of 12.75%.[21]

The DSSC device fabricated with an iminodibenzyl-substituted porphyrin sensitizer[22] yields a J_{SC}

of 9.68 mA.cm^{-2}, V_{OC} of 0.74 V, and FF of 0.73, corresponding to an overall η of up to 5.26%, which is greater than those obtained by diphenylamine- and iminostilbene-substituted porphyrin-sensitized solar cells (η of 4.05% and 2.62%).

Other reports have highlighted that the *meso*-position of the porphyrin plays an active role through various anchoring groups[23] and those dyes act as better sensitizers in DSSCs. For the ZnPors with different combinations of thienyl and *p*-carboxyphenyl groups, were found that the number and the position of these *meso*-substituents in the macrocycle core, significantly affect the performance of the device. The *meso*-*p*-carboxyphenyl substituted Por influences the interfacial electron interaction between trapping electrons and triiodides, and others, like the thienyl, alters the excited-state lifetime of the porphyrin.[24]

The prolonged light exposure effect on the photovoltaic parameters has been reported for various dye sensitized systems.[25-27] Wang *et al.* reported the redistribution of localized states within the

TiO_2 conduction band leading to a conduction-band (CB) shift of the TiO_2 in solar cells sensitized with ruthenium bipyridyl complex Z907.[28] The improvement in efficiency, depending on the electrolyte used, was only moderate. Gregg *et al*. reported a significant (45-fold) increase in the performance of perylene-sensitized DSSCs upon exposure to UV light, which was also explained by a shift of the CB of TiO_2 and improved injection.[29]

Here, we report the study of four ZnPors **a**-**d** (Fig. 1) as photosensitizers in DSSCs, bearing different *meso*-substituents like pyridyl, phenyl and carboxyphenyl acid groups. The ZnPors **a-d** with the corresponding anchoring groups were adsorbed on the semiconductor TiO_2 and the photovoltaic parameters were fully examined, such as current density (J_{sc}, $mA.cm^{-2}$), open-circuit potential (V_{oc}, V), fill factor (FF), and overall solar energy conversion efficiency (η%).

2. Experimental

The synthesis of all studied ZnPors: *meso*-tetrakis(4-pyridyl)porphyrinato Zn(II) (**a**); *meso*-triphenyl(4-carboxyphenyl)porphyrinato Zn(II) (**b**); *meso*-tetrakis(4-carboxyphenyl)porphyrinato Zn(II) (**c**) and *meso*-tripyridyl(4-carboxyphenyl)porphyrinato Zn(II) (**d**) were performed using previously published procedures.[30] The structures of these metalloporphyrins are depicted in figure 1.

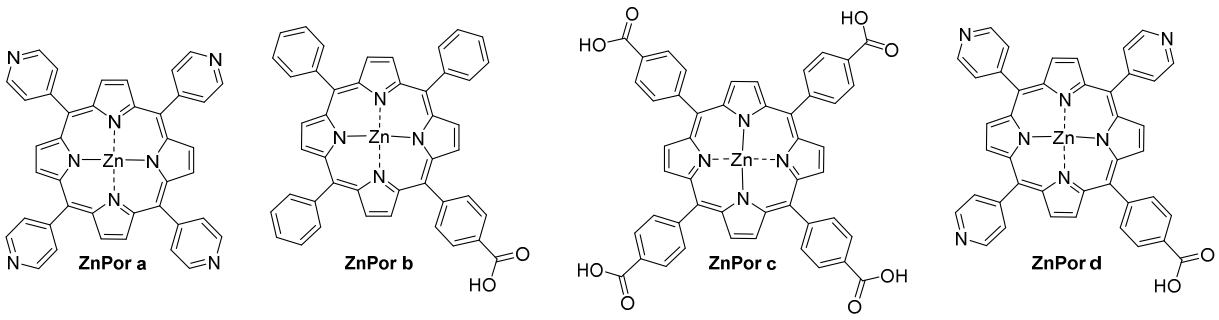

Figure 1 Molecular structures of ZnPors **a-d**.

2.1 Materials and Instruments

The UV-Vis absorption spectra of the solutions and the dyes adsorbed to TiO_2 in transmittance mode were recorded by a Varian Cary 5000. All the spectra were collected at room temperature.

2.2 DSSCs fabrication and photovoltaic characterization

The overall power conversion efficiency of a photovoltaic device is one of the most important parameters in solar cell research, and is defined by the short-circuit photocurrent density (J_{sc}), the open circuit photovoltage (V_{oc}), the fill factor (FF), and the incident light power (P_{in}):

$$\eta = \frac{JscVocFF}{Pin}$$

The conductive fluorine tin oxide FTO-glass (TEC7, Greatcell Solar) used for the preparation of the transparent electrodes was first cleaned with detergent and then washed with water and ethanol. To prepare the anodes, the conductive glass plates were immersed in a $TiCl_4$/water solution (40 mM) at 70 °C for 30 min, washed with water and ethanol and sintered at 500 °C for 30 min. The TiO_2 nanocrystalline layers were deposited on the FTO plates by screen-printing the transparent titania paste (18NR-T, Greatcell Solar) using a frame with polyester fibers having 43.80 mesh per cm^2. This procedure, involving two steps (coating and drying at 125 °C), was repeated two times. The TiO_2 coated plates were gradually heated up to 325 °C, then the temperature was increased to 375 °C in 5 min, and afterwards to 500 °C. The plates were sintered at this temperature for 15 min, and finally cooled down to room temperature. Afterwards the TiO_2 film was treated with the same $TiCl_4$/water solution (40 mM), following the procedure

previously described. A coating of reflector titania paste (WER2-O, Greatcell Solar) was deposited by screen-printing and sintered at 500 °C. Each anode was cut into rectangular pieces (area: 2 cm × 1.5 cm) having a spot area of 0.196 cm^2 with a thickness of 15 μm. The titanium oxide film employed for UV-Vis absorption experiments was prepared by doctor blade: two edges of the glass plate were covered with stripes of an adhesive tape (3 M Magic) in order to obtain a transparent ultrathin TiO_2 film with an estimated thickness of about 6 μm. Dye solutions of the Zn-Pors (0.5 mM) were prepared in methanol and DMSO. The photoanodes were prepared by soaking the screen-printed glasses overnight (~15 h) in the different dye solutions, at room temperature in the dark. The excess dye was removed by rinsing the photoanodes with the same solvent as that employed in the dye solution.

Each counter-electrode consisted of an FTO-glass plate (area: 2 cm × 2 cm) in which a hole (1.5 mm diameter) was drilled. The perforated substrates were washed and cleaned with water and ethanol in order to remove any residual glass powder and organic contaminants. The Pt transparent catalyst (PT1, Greatcell Solar) was deposited on the conductive face of the FTO-glass by doctor blade: one edge of the glass plate was covered with a stripe of an adhesive tape (3 M Magic) both to control the thickness of the film and to mask an electric contact strip. The Pt paste was spread uniformly on the substrate by sliding a glass rod along the tape spacer. The adhesive tape stripe was removed, and the glasses heated at 550 °C for 30 min. The photoanode and the Pt counter-electrode were assembled into a sandwich type arrangement and sealed (using a thermopress) with a hot melt gasket made of Surlyn ionomer (Meltonix 1170-25, Solaronix SA).

The electrolyte was prepared by dissolving the redox couple, I^-/I_2 (0.8 M LiI and 0.05 M I_2), in acetonitrile/valeronitrile (85:15, v/v) mixture. The electrolyte was introduced into the cell *via*

backfilling under vacuum through a hole in the back of the cathode. Finally, the hole was sealed with adhesive tape.

For each compound, three cells were assembled under the same conditions, and the efficiencies were measured from 6 to 14 times for each one.

Here, it is important to highlight the fact that the operating conditions are the most rudimentary and simple, in terms of electrolyte efficiency, sealing methods for DSSC assembling and co-sensitization processes. As such, the photovoltaic performances are relatively low, if compared with the used benchmark N719 dye.

3. Results and Discussion

3.1 Absorption behavior of dyes

The studied metalloporphyrins have strong Soret band intensities at around 425−428 nm and two Q bands between 500−630 nm shown in figure 2, which are spectral characteristics of metalloporphyrins that makes them potential candidates for light harvesting in DSSCs.

Figure 2b presents the absorption spectra of porphyrins adsorbed on a TiO_2 film, showing that Q bands of porphyrin/TiO_2 films are slightly red shifted and become broader compared to the spectra of the solutions in the same solvent (Figure 2a). The broadening of the optical absorption spectra and its red shifting are indications of adsorption interaction between the dye and the semiconductor surface.

Films with coating thickness of around 1 μm were immersed in solutions of ZnPors for 12 h and rinsed with the solvent of the solution to remove unabsorbed dye.

The most straightforward way to increase photocurrent density, J_{sc}, is to absorb a greater fraction of the incident light. Extending the absorption of the dye into the near infrared is an option for increasing the photocurrent density. From the tested ZnPors, the ZnPor **d** showed the highest absorption red-shift upon TiO_2 adsorption with the value of 8 nm. This fact may contribute to a higher photoconversion efficiency observed for DSSC device of ZnPor **d** (Table 1). This observation agrees with the overall DSSC performance and will be further discussed.

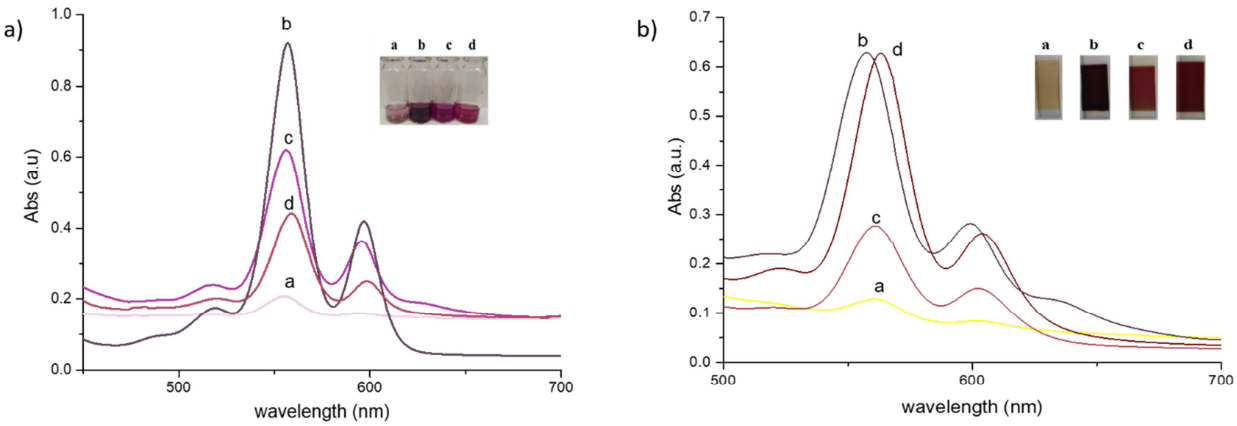

Figure 2 Visible absorption spectra of a) solutions (inset) of 1.25×10^{-4} M in methanol (ZnPors **a-c**) and DMSO (ZnPors **d**) and b) when adsorbed on a 6 μm TiO_2 film (inset) from solutions of 5×10^{-4} M (inset). Presentation of the Soret bands were ignored for clarity.

Table 1 Absorption wavelength (nm) in solution and when adsorbed on a 6 μm TiO_2 film and molar extinction coefficients ε ($M^{-1}cm^{-1}$)).

Compound	Q bands in solution	Log (ε)	Q bands on a TiO_2 film
a	556	4.3	562
	590	3.4	600

b	557	4.3	558
	596	3.8	600
c	558	4.4	561
	598	3.9	603
d	560	4.4	564
	599	3.8	605

3.2 Photovoltaic Performance of DSSC with Iodine-Based Electrolyte

For future practical applications of DSSCs, the long-term efficiency is extremely important, which is highly dependent on the binding ability of the anchoring group of the sensitizers. The most commonly used anchoring groups are highly efficient electron acceptors like derivatives of benzoic acid and cyanoacrylic acid. Despite lower DSSCs efficiencies long term stability and durability have been achieved more effectively when alternative anchoring groups are used like 8-hydroxylquinolin, tropolone, hydroxamic acid, triethoxysilyl and pyridyl-based anchors.[31]

The photocurrent–voltage (*J*-*V*) plots for DSSCs assembled ZnPors **a**-**d** are shown in figure 3, and the photovoltaic performance parameters are presented in table 2. Here, we present the best performing results after a sequence of several consecutive measurements.

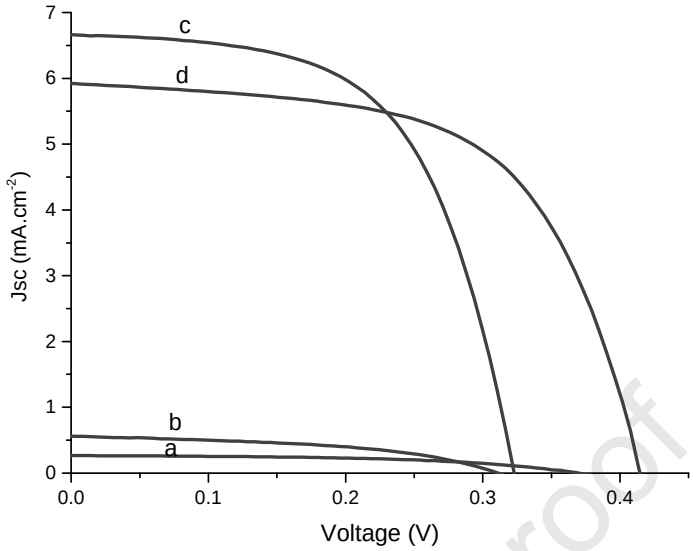

Figure 3 Photocurrent-voltage (*J*-*V*) curves of DSSCs based on ZnPors **a-d** measured under AM 1.5 solar light (100 mW.cm^{-2}), using 0.8 M LiI and 0.05 M I_2 in acetonitrile:valeronitrile (85:15, v/v) as electrolyte.

V_{oc} is the difference between the redox level of the electrolyte and the quasi-Fermi level of the semiconductor; it can be affected by the concentration of electrons in the conduction band (CB) of the semiconductor and the magnitude of electron recombination from the injected dyes to the oxidized electrolyte.[32,33]

ZnPor **a** achieved the lowest photovoltaic performance, that can be explained by the low loading and a lower electron-injection efficiency due to a very scarce interaction between pyridyl group and TiO_2 surface.[34,35] Despite the presence of four pyridyl groups, previously described as able to establish coordination bonds between the nitrogen atom and the Lewis acidic sites of the TiO_2 surface, leading to efficient electron injection,[36] in our case this previously reported result was not observed. As seen from figure 3 and table 2, ZnPor **a** presents the lowest photocurrent density (J_{sc} = 0.29 mA.cm^{-2}) and the lowest energy conversion efficiency (η = 0.057%).

The tetracarboxyphenyl *meso*-substituted ZnPor **c**, when compared with the monocarboxyphenyl ZnPor **b**, presented the best cell performance despite the lowest visible light absorption on the anode surface (Figure 2b).

The decreasing trend of cell efficiencies of the studied ZnPors is the following: ZnPor **a** < ZnPor **b** < ZnPor **c** < ZnPor **d**.

A lower V_{oc} is the only photovoltaic parameter that inhibits the ZnPor **c** from having the best photoconversion efficiency (η, %). In solution, a higher acidic character of ZnPor **c**, due to the presence of a higher number of acidic groups, may affect the band structure at the interface due to the protonation of the TiO_2 surface, as the accumulation of positive charge at the interface results in a lowering of the TiO_2 conduction bands.[37] Also, and as consequence, a larger J_{sc} value due to the driving force for the electron transfer from the LUMO of the dye to the conduction band of TiO_2 is usually observed.[38]

Table 2 Photovoltaic performance parameters of DSSCs based on ZnPors **a**-**d** under 100 $mW.cm^{-2}$ simulated AM 1.5 illumination. The results presented are for the best performing cell and N719 is the benchmark.

ZnPors	V_{oc} (V)	J_{sc} ($mA.cm^{-2}$)	FF	η (%)
a	0.37	0.29	0.59	0.057
b	0.41	0.65	0.52	0.14
c	0.32	6.63	0.59	1.28
d	0.41	5.92	0.60	1.49
N719	0.44	18.5	0.53	4.44

In the present study only ZnPor **a** has no carboxylic acid group for anchorage, and the TiO_2/dye bond must be exclusively established through coordination bonds from the nitrogen of pyridyl

groups and the Lewis acidic sites of the TiO_2. In some cases, the overall DSSCs performance is comparable to those devices using the carboxylic acid group, although in our experiments this fact was not observed. As can be clearly observed from the very low intensity of the absorption spectra of ZnPor **a**, when absorbed on the TiO_2 film, and from table 2, this dye presented the lowest overall DSSC performance. This was mainly due to a very low short-circuit current density (J_{sc}) which is directly influenced by the amount of light absorption, their intramolecular charge transfer, and the interfacial charge transfer from the dye molecules to the semiconductor substrate.

Carboxylic acid anchoring groups typically act as electron acceptors, given their excellent electron-withdrawing capabilities, that facilitates charge transfer from the dye to the region in the vicinity of the TiO_2 substrate.

ZnPor **b**, with only one carboxylic acid group in the *meso*-position, and three phenyl groups in the remaining positions also presented a very weak performance despite the high loading of the dye on the anode surface (Figure 2b). In this case, the solar energy-to-electricity conversion yield (η%) is only 0.14%. The reason may be related with the well-known dye-aggregation effect that can be highly promoted in planar dyes; an inherent strong tendency due to small steric hindrance of unsubstituted phenyl groups like in ZnPor **b**.[39] This result does not completely agree with previously reports, which shows that when ZnPors have more than two *p*-carboxyphenyl groups at the *meso*-positions, the absorbance and molecular loading on TiO_2 is increased.[24]

ZnPor **c**, with four benzoic acids in the *meso*-position presented the best short-circuit current density (J_{sc}) of 4.70 mA/cm^2, corresponding to the first measurement, which improved in 40% after light exposure of almost 5 min, reaching the final value of 6.60 mA.cm^{-2}. It is important to compare these results in parallel to the photovoltaic performance parameters obtained for device

ZnPor **d**. For ZnPor **d**, with a single electron-withdrawing anchoring group and three pyridyl units in the other *meso*-positions, the first J_{sc} measurement presented the value of 4.50 $mA.cm^{-2}$, with improvement upon light exposure until 5.92 $mA.cm^{-2}$ that corresponds to an increase of 31%. A considerably lower V_{oc} was observed for ZnPor **c** which may be associated with a positive shift of the conduction band edge induced by the presence of higher concentration of H^+, due to the presence of four carboxyphenyl groups.

3.2 Light exposure effect

It is frequently reported that continuous light exposure of the device provides a way to significantly and irreversibly improve solar cells efficiency.[25,34,40]

Herein, we also report a significant performance improvement of these metalloporphyrins when exposed to consecutive short periods of white light illumination. Each device testing comprises a period of 16 s of continuous light, time after which photovoltaic parameters were determined.

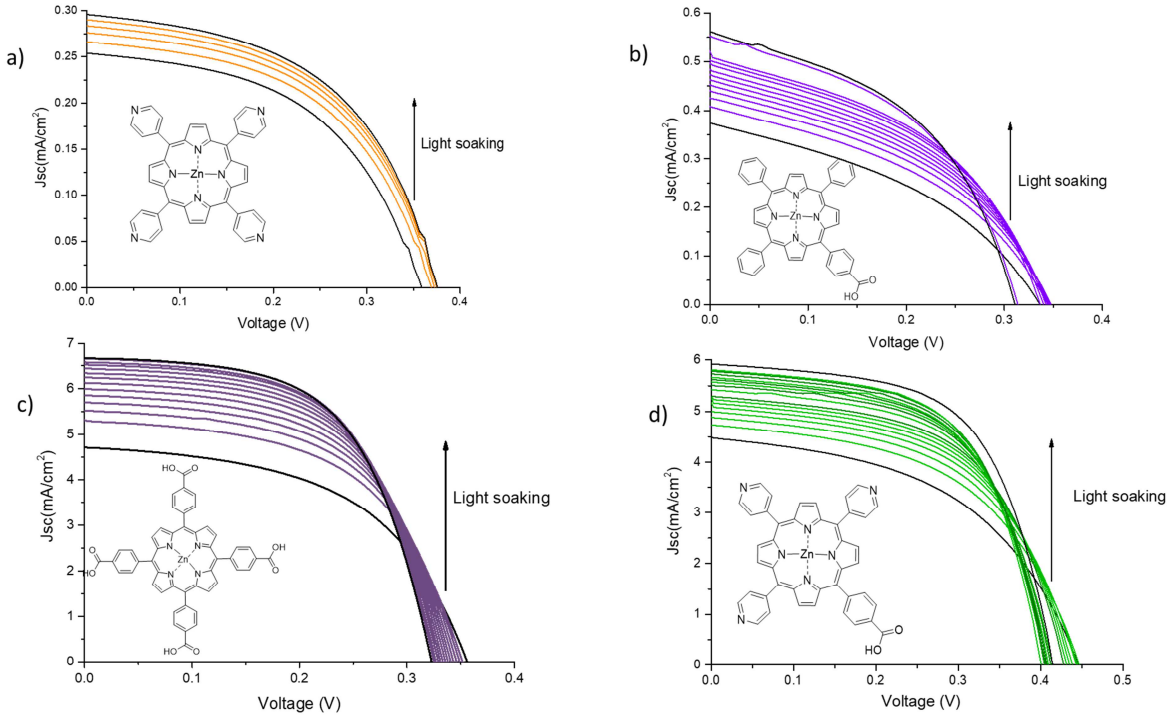

Figure 4 *J-V* graph of photovoltaic performances of DSSCs of ZnPors **a**-**d** upon successive light exposure (16 s each) under full simulated AM 1.5 spectrum.

Devices with ZnPor **b**, ZnPor **c** and ZnPor **d** improve significantly the short-circuit density (J_{sc}) with the same order of magnitude, close to 40% upon a sequence of several consecutive measurements (Table 3). The J_{sc} of device assembled with ZnPor **a** improved only 11% reaching the plateau after a sequence of only six acquisitions.

Table 3 ZnPors **a-d** DSSCs device parameters before (first value) and after (second value) light exposure between 1 to 5 min.

ZnPors	V_{OC} (V)	J_{SC} (mA.cm^{-2})	FF	η (%)
a	0.36/0.37	0.25/0.29	50.3/50.9	0.046/0.057
b	0.40/0.41	0.52/0.65	46.8/51.9	0.099/0.14
c	0.36/0.32	4.20/6.63	49.9/58.7	0.76/1.28
d	0.44/0.41	4.99/0.41	53.3/60.6	1.19/1.49

Contrasting with devices ZnPor **b**, ZnPor **c** and ZnPor **d**, DSSC assembled with porphyrin ZnPor **a**, presented a discreet improvement in the photovoltaic open circuit voltage (V_{oc}). A structural feature of ZnPor **a** that could explain this observation, is that it has no carboxylic acid anchoring group and the *meso*-positions are filled with four pyridyl units.

The reduction of V_{oc} could then be related with the fact that light exposure promotes carboxylic acid deprotonation with concomitant improvement in the degree of anchoring. For the same reason higher concentration of H^+, that are readily adsorbed onto the TiO_2 electrode induce a downward shift in the Fermi level; hence a drop in V_{oc} occurs due to the positive shift of the conduction band edge induced by the presence of surface H^+.[37] This may explain the tendency of 6, 11, and 9% decrease in V_{oc} respectively for ZnPor **b**, ZnPor **c** and ZnPor **d** upon device light exposure for approximately 3-5 min (Figure 5).

Despite V_{oc} lowering, the same phenomena may contribute to a better charge transfer from the dye molecules to the semiconductor substrate, reflecting then an improvement in short-circuit photocurrent density, J_{sc}, as was observed in ZnPor **b-d**.[37,38]

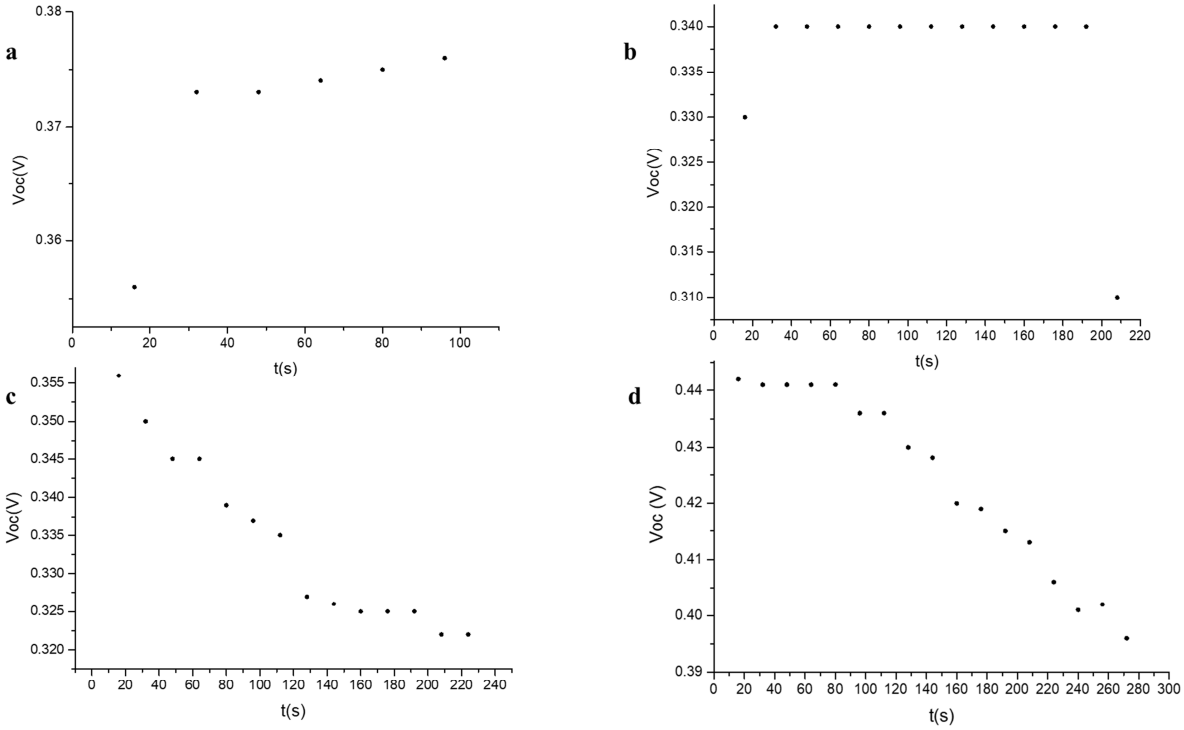

Figure 5 Open-circuit voltage (V_{oc}) *versus* time exposure to solar simulator light.

Considering the possibility of dual point of anchorage, more information is obtained when pyridyl and carboxylic acid interact with semiconductor surface. To elucidate the adsorption modes of ZnPor **d** at TiO_2 nanoparticles, the FTIR spectra of the dyes as a powder was measured when adsorbed on TiO_2 nanoparticles and also after sensitization on TiO_2 films, obtained by dis-assembling device ZnPor **d** after 5 min under white light exposure (Figure 6).

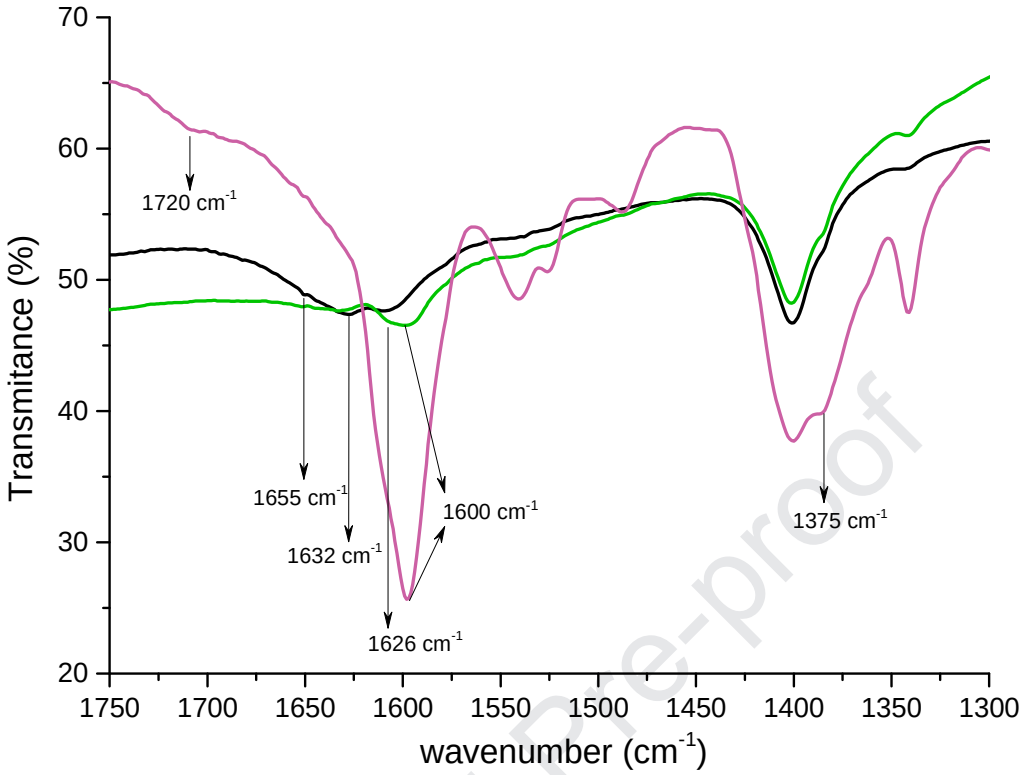

Figure 6 FTIR spectra of dye ZnPor **d** powder (purple line), ZnPor **d** adsorbed on the TiO_2 surface (green line) and TiO_2/dye ZnPor **d** film disassembled after almost 5 min of light exposure (black line).

Generally, with few exceptions, ZnPor **d** powder FTIR absorption bands are maintained after adsorption on the TiO_2 surface. This includes the characteristic stretching bands for C=N or C=C observed at around 1541, 1525, and 1487 cm^{-1} for all the dye powders.

The FTIR spectra of the ZnPor **d** display the distinctive band of ν(C=O) of the carboxylic acid around 1720 cm^{-1} (shoulder). On the other hand, the FTIR spectra of ZnPor **d**/TiO_2 and the disassembled ZnPor **d**/TiO_2, after light exposure, exhibited a disappearance of the ν(C=O) band around 1720 cm^{-1} as well as a considerable relative decrease in the intensity of vibrational energy of the symmetric carboxylate absorption, ν(COO−sym), close to 1375 cm^{-1}.[43]

The adsorption of the pyridyl group onto the Lewis acidic surface of TiO_2 was evident from the emerging vibrational band at 1626 cm^{-1}, when ZnPor **b** is adsorbed on the TiO_2 surface.[41,42] After device disassembling upon light exposure, one new band appear at 1655 cm^{-1}, and the band at 1632 cm^{-1} increases in intensity attributed to Brønsted acidic of TiO_2 sites bonded to the pyridyl groups.[43]

Conclusions

In summary, we have presented and discussed some aspects of four *meso*-substituted porphyrins, particularly the effect on the photovoltaic performance in DSSC considering the number of *p*-carboxyphenyl anchoring groups. Also, we were not able to observe the anchoring character of pyridyl *meso*-substituent, unless the presence of at least one *p*-carboxyphenyl group is available in the porphyrin structure.

The best photovoltaic performance was observed for the device ZnPor **d**/TiO_2 where the combination of the pyridyl and carboxyphenyl acid groups appear to have a dual anchoring to TiO_2 surface. This dual anchor was more evidently observed after the light exposure under full simulated AM 1.5 spectrum. ZnPor **d** seems to have the best combination of the different *meso*-substituent groups.

The significant and simultaneous improvement in device parameters under solar simulator light illumination of porphyrin-sensitized solar cells, suggests a complex phenomenon. Changes to the dye binding modes closer to the FTO surface, however, cannot be ruled out, taking in consideration the FTIR analysis before and after light exposure of the device.

Future work demands exploring this feature as a mean of significantly increase photoconversion efficiencies of porphyrin dyes.

Acknowledgments

Thanks are due to FCT/MCTES for the financial support to QOPNA (FCT UID/QUI/00062/2019), Centro de Química Estrutural (UIDB/00100/2020) and LAQV-REQUIMTE (UIDB/50006/2020) research units, and to PTDC/QUI-QOR/31770/2017 and P2020-PTDC/QEQ-SUP/5355/2014 research grants to L. Lourenço, through national founds (PIDDAC) and where applicable co-financed by the FEDER-Operational Thematic Program for Competitiveness and Internationalization-COMPETE 2020, within the PT2020 Partnership Agreement. J. Calmeiro thanks FCT for the research fellow BI/UI51/7955/2019. S. Fernandes and A. Pinto thank FCT for their Ph.D. scholarships SFRH/BD/129200/2017 and PD/BD/135087/2017, respectively. C. Pereira thanks FCT for the Norma Transitória DL 57/2016 Program Contract.

References

[1] M. S. Suait, M. Y. A. Rahman, A. Ahmad, *Sol. Energy*, **2015**, 115, 452–470.

[2] Enerda, "Share of renewables in electricity production," 2019. [Online]. Available: https://yearbook.enerdata.net/renewables/renewable-in-electricity-production-share.html. [Accessed: 28-Oct-2019].

[3] a) L. Wibmer, L. M. O. Lourenço, A. Roth, G. Katsukis, M. G. P. M. S. Neves, J. A. S. Cavaleiro, J. P. C. Tomé, T. Torres, D. M. Guldi, *Nanoscale* **2015**, 7, 5674–5682. b) L. M O. Lourenço, A. Hausmann, C. Schubert, M. G. P. M. S. Neves, J. A. S. Cavaleiro, T. Torres, D. M. Guldi, J. P. C. Tomé, *ChemPlusChem* **2015**, 80, 832–838.

[4] N. Robertson, *Angew.Chem. Int.Ed.* **2006**, 45, 2338–2345.

[5] a) B. O'Regan, M. Grätzel, *Nature* **1991**, 353, 737–739. b) G. de La Torre, W. Blau, T. Torres, *Nanotechnology* **2003**, 14, 765–771. c)M. Grätzel, *Inorg. Chem.* **2005**, 44, 6841–6851. d) J. R. Pinzûn, M. E. Plonska-Brzezinska, C. M. Cardona, A. J. Athans, S. S. Gayathri, D. M. Guldi, M. A. Herranz, N. Martin, T. Torres, L. Echegoyen, *Angew. Chem. Int. Ed.* **2008**, 47, 4173–4176. e) M. Quintiliani, A. Kahnt, T. Wçlfle, W. Hieringer, P. Vazquez, A. Gçrling, D. M. Guldi, T. Torres, *Chem. Eur. J.* **2008**, 14, 3765–3775. f) H. Gommans, T. Aernouts, B. Verreet, P. Heremans, A. Medina, C. G. Claessens, T. Torres, *Adv. Funct. Mater*. **2009**, 19, 3435–3439.

[6] G. Richhariya, A. Kumara, P. Tekasakul, B. Gupta, *Renew Sust Energ Rev* **2017**, 69, 705–718.

[7] G. Calogero, J.-H. Yum, A. Sinopoli, G. Di Marco, M. Grätzel, M. K. Nazeeruddin, *Sol Energy* **2012**, 86, 1563–1575

[8] A. L. Pinto, L. Cruz, V. Gomes, H. Cruz, G. Calogero, V. de Freitas, F. Pina, A. J. Parola, J. C. Lima, *Dyes Pigm.* **2019**, 170, 107577–107584.

[9] A. L. Pinto, J. Oliveira, P. Araújo, G. Calogero, V. de Freitas, F. Pina, A. Jorge Parola, J. C. Lima, *Solar Energy* **2019**, 191, 100–108.

[10] G. Calogero, I. Citro, C. Crupi, G. Carini Jr, D. Arigò, G. Spinella, A. Bartolotta, G. Di Marco *Opt. Mater.* **2019**, 88, 24–29.

[11] a) W. M. Campbell, K. W. Jolley, P. Wagner, K. Wagner, P. J. Walsh, K. C. Gordon, L. Schmidt-Mende, M. K. Nazeeruddin, Q. Wang, M. Grätzel, D. L. Officer *J. Phys. Chem. C.* **2007**, 111, 11760–11762. b) M. G. Walter, A. B. Rudine, C. C. Wamser, *J. Porphyrins Phthalocyanines* **2010**, 14, 759–792. c) L. Li, E. W. Diau, *Chem. Soc. Rev.* **2013**; 42, 291–304.

[12] a) A. S. Hart, C. B. KC, H. B. Gobeze, L. R. Sequeira, F. D'Souza, *ACS Appl. Mater. Interfaces.* **2013**, 5, 5314–5323. b) B. J. Brennan, M. J. L. Portlés, P. A. Liddell, T. A. Moore, A. L. Moore, D. Gust, *Phys. Chem. Chem. Phys.* **2013**, 15, 16605–16614.

[13] L. Etgar, *Materials* **2013**, 6, 445–459.

[14] a) I. Zegkinoglou, M. Ragoussi, C. D. Pemmaraju, P. S. Johnson, D. F. Pickup, J. E. Ortega, D. Prendergast, G. de la Torre, F. J. Himpsel, *J. Phys. Chem. C*. **2013**, 117, 13357–13364.

[15] a) A. N. M. Green, E. Palomares, S. A. Haque, J. M. Kroon, J. R. Durrant, *J. Phys. Chem. B.* **2005**, 109, 12525–12533. b) E. M. Barea, J. Ortiz, F. J. Payá, F. Fernández-Lázaro, F. Fabregat-Santiago, A. Sastre-Santos, J. Bisquert, *J. Energy Environ. Sci*. **2010**, 3, 1985–1994. c) S. M. Feldt, P. W. Lohse, F. Kessler, M. K. Nazeeruddin, M. Grätzel, G. Boschloo, A. Hagfeldt, *Phys. Chem. Chem. Phys*. **2013**, 15, 7087–7097.

[16] a) A. Mishra, M. K. R. Dipl.-Chem., P. Bäuerle, *Angew. Chem., Int. Ed.* **2009**, 48, 2474–2499. b) A. Kira, Y. Matsubara, H. Lijima, T. Umeyama, Y. Matano, S. Ito, M. Niemi, N. V. Tkachenko, H. Lemmetyinen, H. Imahori, *J. Phys. Chem. C* **2010**, 114, 11293–11304. c) D.

Daphnomili, G. Landrou, S. P. Singh, A. Thomas, K. Yesudas, B.K., G. D. Sharma, A. G. Coutsolelos, *RSC Advances* **2012**, 2, 12899–12908.

[17] M. Urbani, M. Gratzel, M. K. Nazeeruddin, T. Torres, *Chem. Rev.* **2014**, 114, 12330−12396.

[18] F. Odobel, Y. Pellegrin, J. Warnan, *Energy Environ. Sci*. **2013**, 6, 2041–2052.

[19] a) S. Mathew, A. Yella, P. Gao, R. Humphry-Baker, F. E. C. Basile, N. Ashari-Astani, I. Tavernelli, U. Rothlisberger, M. K. Nazeeruddin, M. Gratzel, *Nat. Chem.* **2014**, 6, 242–247. b) T. Bessho, S. M. Zakeeruddin, C. Y. Yeh, E. W. G. Diau, M. Gratzel, *Angew. Chem., Int. Ed.* **2010**, *49*, 6646–6649. c) A. Yella, H. W. Lee, H. N. Tsao, C. Yi, A. K. Chandiran, M. K. Nazeeruddin, E. W. G. Diau, C. Y. Yeh, S. M. Zakeeruddin, M. Gratzel, *Science* **2011**, 334, 629–634. d) J. W. Shiu, Y. C. Chang, C. Y. Chan, H. P. Wu, H. Y. Hsu, C. L. Wang, C. Y. Lin, E. W. G. Diau, *J. Mater. Chem. A*, **2015**, 3, 1417–1420.

e) J. Luo, M. Xu, R. Li, K. W. Huang, C. Jiang, Q. Qi, W. Zeng, J. Zhang, C. Chi, P. Wang, Wu, *J. Am. Chem. Soc*. **2014**, 136, 265–272. f) T. Higashino, Y. Fujimori, K. Sugiura, Y. Tsuji, S. Ito, H. Imahori, *Angew. Chem., Int. Ed*. **2015**, 54, 9052–9056.

g) S. H. Kang, M. J. Jeong, Y. K. Eom, I. T. Choi, S. M. Kwon, Y. Yoo, J. Kim, J. Kwon, J. H. Park, H. K. Kim, *Adv. Energy Mater.* **2017**, 7, 1602117.

[20] A. Yella, H.-W. Lee, H. N. Tsao, C. Yi, A. K. Chandiran, Md.K. Nazeeruddin, E. W-G. Diau, C.-Y. Yeh, S. M. Zakeeruddin, M. Grätzel, *Science* **2011**, 334, 629–334.

[21] A. Yella, C. L. Mai, S. M. Zakeeruddin, S. N. Chang, C. H. Hsieh, C. Y. Yeh and M. Grätzel, *Angew. Chemie - Int. Ed.*, **2014**, 53, 2973–2977.

[22] Y. Liang, X. Xue, W. Zhang, C. Fan, Y. Li, B. Zhang, Y. Feng, *Dye. Pigm.*, **2014**, 115, 7–16.

[23] L. M. O. Lourenço, J. Resende, B. A. Iglesias, K. Castro, S. Nakagaki, M. J. Lima, A. F. da Cunha, M. G. P. M. S. Neves, J. A. S. Cavaleiro, J. P. C. Tomé, *J. Porphyrins Phthalocyanines* **2014**, 18, 967–974.

[24] R. Ambre, K.-B. Chen, C.-F. Yao, L. Luo, E. W.-G. Diau, C.-H. Hung, *J. Phys. Chem. C* **2012**, 116, 11907−11916.

[25] Q. Wang, Z. Zhang, S. M. Zakeeruddin, M. Gra1tzel, J. *Phys. Chem. C* **2008**, 112, 7084–7092.

[26] M. J. Griffith, K. Sunahara, A. Furube, A. J. Mozer, D. L. Officer, P. Wagner, G. G. Wallace, S. Mori, *Phys. Chem. C* **2013**, 117, 11885–11898.

[27] K. Wagner, M. J. Griffith, M. James, A. J. Mozer, P. Wagner, G. Triani, D. L. Officer, G. G. Wallace, *J. Phys. Chem. C* **2011**, 115, 317–326.

[28] Q. Wang, Z. Zhang, S. M. Zakeeruddin, M. J. Gratzel, *Phys. Chem. C* **2008**, 112, 7084–7092.

[29] S. Ferrere, B. A. Gregg, *J. Phys. Chem. B* **2001**, 105, 7602–7605.

[30] J. P. C. Tomé, M. G. P. M. S. Neves, A. C. Tomé, J. A. S. Cavaleiro, M. Soncin, M. Magaraggia, S. Ferro, G. Jori, *J. Med. Chem.* **2004**, 47, 6649–6652.

[31] H. Song, Q. Liu, Y. Xie, *Chem. Commun.* **2018**, 54, 1811–1824.

[32] H. J. Snaith, L. Schmidt-Mende, M. Grätzel, M. Chiesa, *Physical Review B* **2006**, 74, 045306-6.

[33] S. R. Raga, E. M. Barea, F. Fabregat-Santiago, *J. Phys. Chem. Lett.* **2012**, 3, 12, 1629–1634

[34] L. Pellejà, C. V. Kumar, J. N. Clifford, E. Palomares, *J. Phys. Chem. C* **2014**, 118, 16504−16509

[35] D. Daphnomili, G. Landrou, S. P. Singh, A. Thomas, K. Yesudas, K. Bhanuprakash, G. D. Sharma, A. G. Coutsolelos, *RSC Adv.* **2012**, 2, 12899–12908.

[36] L. Zhang, J. M. Cole, ACS *Appl. Mater. Interfaces* 2**015**, 7, 3427−3455.

[37] W. R. Duncan, O. V. Prezhdo, *Annu. Rev. Phys. Chem.* **2007**, 58, 143−184.

[38] M. Adineh, P. Tahay, M. Ameri, N. Safari and E. Mohajerani, *RSC Adv*. **2016**, 6, 14512-14521.

[39] L. Zhang, J. M. Cole, *J. Mater. Chem. A* **2017**, 5, 19541–19559.

[40] J. Gao, W. Yang, A. M. El-Zohry, G. K. Prajapati, Y. Fang, J. Dai, Y. Hao, V. Leandri, P. H. Svensson, I. Furó, G. Boschloo, T. Lund, L. Kloo, *J. Mater. Chem. A* **2019**, 7**,** 19495–19505.

[41] V. Vishwanathan, H.-S. Roh, J.-W. Kim, K.-W. Jun, *Catal. Lett.* **2004**, 96, 23–24.

[42] M. M. Mohamed, W. A. Bayoumy, M. Khairy, M. A. Mousa, *Microporous Mesoporous Mater*. **2007**, 103, 174–183.

[43] Y. Ooyama, S. Inoue, T. Nagano, K. Kushimoto, J. Ohshita, I. Imae, K. Komaguchi, Y. Harima, *Angew. Chem. Int. Ed.* **2011**, 50, 7429–7433.

Highlight

Here we present and discuss some aspects of four *meso*-substituted porphyrins, particularly the effect on the photovoltaic performance in DSSC considering the number of *p*-carboxyphenyl anchoring groups. Also, we were able to conclude that anchoring character of pyridyl *meso*-substituent, is observed only in the presence of at least one *p*-carboxyphenyl group in the porphyrin structure.

The significant and simultaneous improvement in all photovoltaic parameters, when exposed to short periods of white light illumination, suggests a complex phenomenon that deserves attention in the near future.

Conflict of interest

There is no conflict of interest to declare

Declaration of interests

☒ The authors declare that they have no known competing financial interests or personal relationships that could have appeared to influence the work reported in this paper.

☐The authors declare the following financial interests/personal relationships which may be considered as potential competing interests: